photonics

MDPI

Communication

Achieving Up-Conversion Amplified Spontaneous Emission through Spin Alignment between Coherent Light-Emitting Excitons in Perovskite Microstructures

Xixiang Zhu [1,2,*], Yulin Xie [3] and Xiaoling Ma [1]

[1] Key Laboratory of Luminescence and Optical Information, Ministry of Education, Department of Physics, School of Physical Science and Engineering, Beijing Jiaotong University, Beijing 100044, China; maxl@bjtu.edu.cn
[2] School of Electronic and Information Engineering, Beijing Jiaotong University, Beijing 100044, China
[3] School of Physics and Electronics, Huanggang Normal University, Huanggang 438000, China; xieyulin@hgnu.edu.cn
* Correspondence: xxzhu@bjtu.edu.cn

Abstract: Metal hybrid perovskites have presented interesting infrared-to-visible up-conversion light-emitting lasing properties through multi-photon absorption. Here, when the optical pumping switches between circular and linear polarization, up-conversion amplified spontaneous emission (ASE) intensity exhibits large and small amplitudes, respectively, leading to a positive up-conversion ΔASE in the $CsPbBr_3$ perovskite microrods. This observed phenomenon demonstrates that the coherent interaction between coherent light-emitting excitons is indeed established at the up-conversion ASE regime in the $CsPbBr_3$ perovskite microrods. In addition, the positive up-conversion ΔASE indicates the orbital magnetic dipoles between coherent light-emitting excitons are conserved during up-conversion ASE action. Essentially, the up-conversion ΔASE results provide evidence that shows up-conversion ASE can be realized by the orbit−orbit polarization interaction between light-emitting excitons. Moreover, up-conversion ASE proportionally increased as the pumping fluence increased, which shows that orbit–orbit polarization interaction can be gradually enhanced between coherent light-emitting excitons by increasing pumping density in the $CsPbBr_3$ perovskite microrods. Substantially, our studies provide a fundamental understanding of the spin alignment between coherent light-emitting excitons towards developing spin-dependent nonlinear lasing actions in metal halide perovskites.

Keywords: light-emitting excitons; ASE; up-conversion; $CsPbBr_3$ microrods

Citation: Zhu, X.; Xie, Y.; Ma, X. Achieving Up-Conversion Amplified Spontaneous Emission through Spin Alignment between Coherent Light-Emitting Excitons in Perovskite Microstructures. *Photonics* **2022**, *9*, 353. https://doi.org/10.3390/photonics9050353

Received: 23 April 2022
Accepted: 12 May 2022
Published: 18 May 2022

1. Introduction

The metal hybrid perovskites have recently attracted widespread attention as promising candidates for solution-processed optoelectronic applications such as photovoltaics [1,2], lasing [3,4], light-emitting diodes [5,6], and photodetectors [7,8], because of the tunable optical bandgap and remarkable charge transport properties [9,10]. The metal hybrid perovskite $APbX_3$ (where A = Cs^+, CH_3NH^{3+}, or $HC(NH_2)^{2+}$; X = Br^-, I^-, and Cl^-) materials with all of these characteristics have been realized in various forms, including thin films, single crystals, nanowires, and quantum dots [11–13]. In particular, $CsPbBr_3$ perovskites have demonstrated the capabilities of generating multi-photon up-conversion amplified spontaneous emission (ASE) through multi-photon absorption under infrared laser excitation [14,15]. This indicates high power laser excitation is necessary to realize the simultaneous absorption of multiple photons through the interaction between incident electromagnetic waves and photo-induced polarizations. In contrast, metal halide perovskites are formed with s-p orbital hybridization in their band structures, leading to strong orbital momentum in light-emitting excitons [16,17]. The orbital momentum provides the precondition to realize the interaction between incident electromagnetic waves

and photoinduced polarizations when electrons are excited by high-power laser excitation, leading to multi-photon absorption up-conversion ASE. Furthermore, our previous work has found that long-range orbital–orbital polarization interactions occur at the generation of ASE in perovskite, which provides the necessary conditions for coherent interactions between light-emitting excitons through polarization-dependent ASE studies [18–22].

In this work, we study the coherent interaction between light-emitting excitons in the up-conversion ASE regime based on $CsPbBr_3$ perovskite microrods upon operating orbital magnetic dipoles by using circularly polarized optical pumping.

2. Materials and Methods

2.1. Materials

The $CsPbBr_3$ precursor solution was prepared by dissolving 0.1 mmol CsBr (Xi'an Polymer Light Technology Corp, Xi'an, China) and $PbBr_2$ (Xi'an Polymer Light Technology Corp, Xi'an, China) into 1 mL dimethylformamide (Sigma-Aldrich, St. Louis, MO, USA). The solution was then subjected to ultrasonic treatment for 10 min. For $CsPbBr_3$ microrod growth process, 2 µL solution was dropped on a pre-cleaned glass substrate. The substrate was then placed into a sealed glass container with an isopropyl alcohol atmosphere for 12 h, in which the $CsPbBr_3$ microrods start to grow. After the growth process was finished, the substrate was rinsed with toluene solvent and dried with a nitrogen gas blow.

2.2. Characterizations

The optical microscopy images were captured using the Horiba Xplora Plus system. The excitation and the photoluminescence (PL) spectra were measured using the Horiba Fluorolog 3 spectrometer with the Xenon lamp as the excitation source. The ASE spectra were recorded using the Oceanoptics FLAME-S-XR1-ES spectrograph. The pump beam was from a pulsed laser beam (1030 nm) generated through a harmonic generator (Ultrafast Systems LLC, Sarasota, FL, USA, third harmonic) with a Pharos laser (Light Conversion, 25 kHz, 1030 nm, 290 fs). The diameter of the focused laser beam was ~100 µm. All the ASE measurements were performed in the transmission geometry with the pump beam and detection direction normal to the sample surface. The time-resolved PL measurements in the ASE regime were taken using the Horiba Fluorolog 3 time-correlated single-photon counting system in combination with the pulsed laser beam (1030 nm, 25 kHz). For the ΔPL measurements in the ASE regime, a linear polarizer combined with the zero-order quarter plate was used to generate a switchable linearly and circularly polarized pump beam with identical intensity.

3. Results

3.1. Optical Characterizations

For optical characterizations, the $CsPbBr_3$ microrods were prepared by a solution process (see Experimental Method). Figure 1a shows the optical microscopy images of the prepared $CsPbBr_3$ microrods. Obviously, $CsPbBr_3$ microrods are rectangular in shape and measure approximately tenths of a millimeter in size. Figure 1b shows the excitation and up-conversion PL spectra of the $CsPbBr_3$ microrods. The up-conversion PL spectrum exhibited a peak at 533 nm with narrow full width at half maximum (FWHM) of 23 nm under 1030 nm pulse laser with a duration of 290 fs at 8.2 mJ/cm^2.

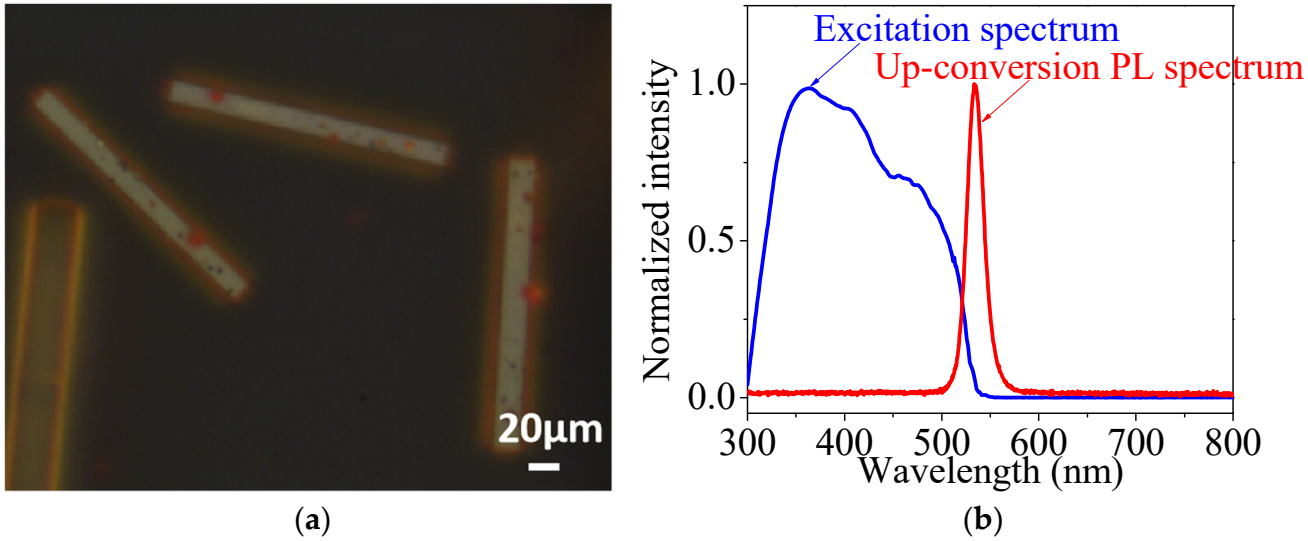

Figure 1. Optical characteristics of CsPbBr3 perovskite microrods: (**a**) optical microscopy image; (**b**) excitation spectrum with emission at 533 nm and up-conversion PL spectrum under 1030 pulse laser excitation.

3.2. Up-Conversion ASE Emission Spectra

Figure 2a shows the up-conversion emission spectra from the $CsPbBr_3$ microrods under 1030 nm pulse laser with a duration of 290 fs at different pumping intensities. A narrow up-conversion emission peak at 543 nm was observed when the pumping power reached 14.3 mJ/cm^2. We should note that a narrow up-conversion red-shifted ASE peak appearing along with the increased excitation power can be attributed to the waveguided photons' reabsorption with the reduced optical loss [23,24]. Figure 2b demonstrates the spectral intensity and width as a function of pumping power. The up-conversion emission intensity was increased greatly along with the FWHM being decreased to approximately 14 nm when the pumping power was gradually increased above the threshold of 14.3 mJ/cm^2. Here, it is observed the power dependence with the slope of 1.7 indicates that the up-conversion PL undergoes a two-photon process when the excitation power is below the threshold. Figure 2c shows the time-resolved PL lifetimes of up-conversion ASE peaked at 543 nm and up-conversion spontaneous emission peaked at 533 nm when the pumping power is above the threshold of 14.3 mJ/cm^2. It can be seen that up-conversion ASE decays much faster than the up-conversion spontaneous emission. The fast decay shows a stimulated light-emitting process within the ASE region when the pumping power exceed a threshold of 14.3 mJ/cm^2. Especially, we should note that the realization of ASE needs to satisfy two conditions: (i) polarizing the light-emitting excitons before radiative emission occurs and (ii) initiating the coherent interaction between light-emitting excitons, leading to coherent light-emitting states. Therefore, our up-conversion ASE results indicate a coherent interaction between light-emitting excitons is established during up-conversion ASE action in the CsPbBr3 perovskite microrods.

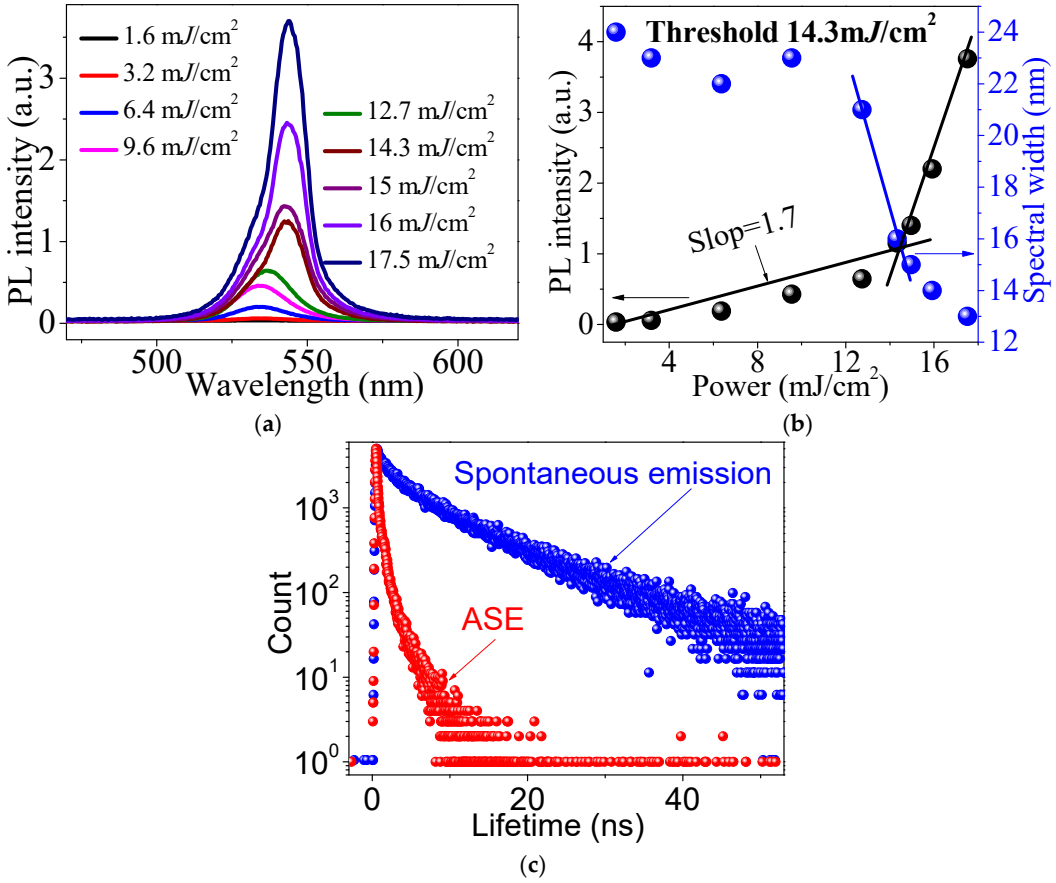

Figure 2. Up-conversion emission spectral characteristics in CsPbBr3 nanorods under 1030 nm pulse laser excitation: (**a**) PL spectra under different pump fluences measured in transmission mode; (**b**) FWHM and up-conversion ASE intensity against pumping power; (**c**) decay curves.

4. Discussion

We now discuss the spin alignment between coherent light-emitting excitons at the up-conversion ASE regime in $CsPbBr_3$ perovskite microrods. Figure 3 shows the up-conversion ASE (peaked at 543 nm) and up-conversion PL (peaked at 533 nm) intensities when the 1030 nm pumping beam is transitioned between linear and circular polarization at the same intensity in the $CsPbBr_3$ microrods. Here, the up-conversion ΔASE is defined by $\Delta ASE = \frac{I_{Circular} - I_{Linear}}{I_{Linear}}$, where I_{Linear} and $I_{Circular}$ are the up-conversion ASE intensities under linearly and circularly polarized photoexcitation, respectively. When increasing pumping fluence above the threshold of 15 mJ/cm^2, the positive up-conversion ΔASE with the amplitude of 11% can be observed by switching circularly and linearly polarized pumping, as shown in Figure 3a. Furthermore, the PL intensity remains virtually unchanged upon switching the pumping between linear and circular polarization in the up-conversion spontaneous emission region. This up-conversion ΔASE phenomenon provides three experimental indications. First, the relaxation of aligned orbital magnetic dipoles between coherent light-emitting excitons reaches 8 ns at room temperature, comparable with the up-conversion ASE. This satisfies the precondition to use the up-conversion ΔASE phenomenon to identify the spin alignment between coherent light-emitting excitons. Second, the observed up-conversion ΔASE phenomenon indicates that the spin alignment is realized by optically generating the same-directional orbital magnetic dipoles under circularly polarized pumping, leading to a coherent interaction between coherent light-emitting excitons through orbit–orbit polarization interaction. Third, the positive ΔASE caused by switching the pumping beam from linear to circular polarization indicates that the spin alignment indeed introduces an additional coherent interaction between transition dipoles

through in-phase orbital polarization between coherent light-emitting excitons. Clearly, by monitoring the up-conversion ASE intensity when the pumping beam switched between linear and circular polarization, the spin-polarized coherent light-emitting excitons are indeed established through orbit–orbit polarization interaction during the up-conversion ASE in $CsPbBr_3$ perovskite microrods. Moreover, up-conversion ΔASE is proportionally increased from 14% to 17% when the pumping power is increased from 16 mJ/cm^2 to 17 mJ/cm^2. In addition, the PL intensity keeps constant upon switching the pumping between linear and circular polarization in the up-conversion spontaneous emission region. This indicates that the coherent interaction between coherent light-emitting excitons is largely increased by increasing pumping density within up-conversion ASE regime in the $CsPbBr_3$ microrods. It should be noted that establishing coherent transition dipoles and spin alignment requires different threshold pumping intensities. The coherent transition dipoles are established at a lower threshold pumping power of 14.7 mJ/cm^2, initiating a spectral narrowing phenomenon (Figure 2b). When the excitation reached a higher threshold pumping power of 15 mJ/cm^2, up-conversion ΔASE can be realized by establishing the spin alignment between coherent transition dipoles (Figure 3). Clearly, when the density of coherent transition dipoles is increased, the spin alignment between coherent transition dipoles can be gradually established by increasing the pumping power of circular polarization, leading to increasing coherent interaction between light-emitting excitons in the $CsPbBr_3$ microrods.

Here, we monitor the up-conversion ASE amplitude by switching the optical pumping beam between linear and circular polarization. Clearly, in the $CsPbBr_3$ perovskite microrods, circularly polarized excitation produced higher up-conversion ASE than linearly polarized excitation with the same pumping power, leading to positive up-conversion ΔASE phenomenon at room temperature. Furthermore, up-conversion ΔASE magnitude proportionally increased with increasing excitation power. This result indicates that spin-polarized coherent light-emitting excitons are indeed generated and also enhanced with the increasing excitation power in the $CsPbBr_3$ perovskite microrods, leading to up-conversion ASE. Essentially, this indicates that under the action of a circularly polarized light pump, the aligned magnetic dipole can form an in-phase transition dipole between light-emitting excitons, thus forming spin-polarized coherent optical excitons during nonlinear optical actions in $CsPbBr_3$ perovskite microrods.

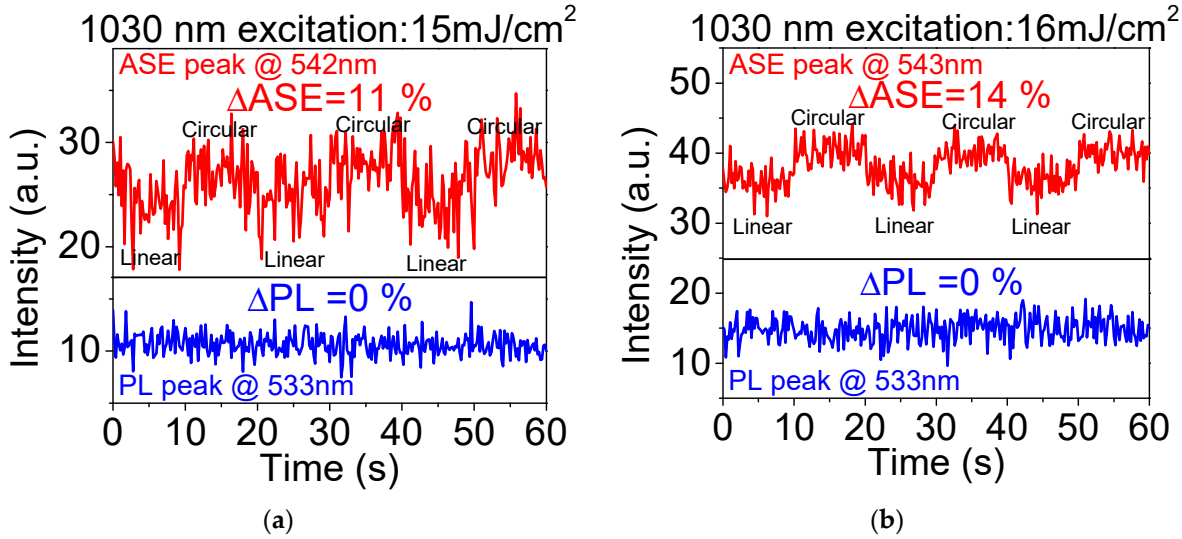

(**a**) (**b**)

Figure 3. *Cont.*

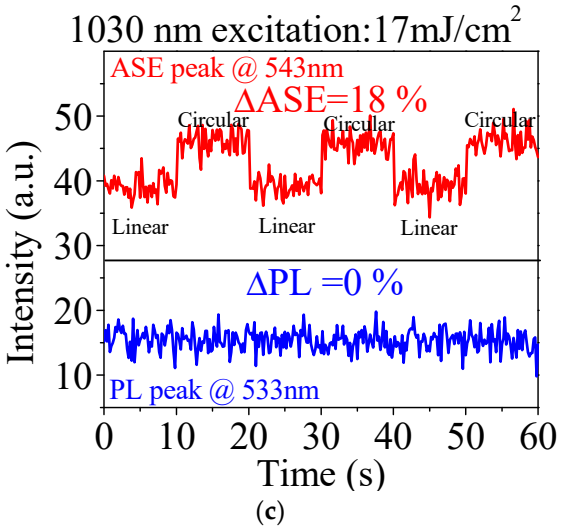

Figure 3. Up-conversion PL intensities at ASE peak (543 nm) and PL peak (533 nm) under linear and circular photoexcitation with different excitation power of 1030 nm pulse laser in $CsPbBr_3$ nanorods: (**a**) pumping power: 15 mJ/cm^2; (**b**) pumping power: 16 mJ/cm^2; (**c**) pumping power: 17 mJ/cm^2.

5. Conclusions

In summary, by monitoring up-conversion ΔASE when switching the pump beam between linear and circular polarization, we found that the coherent interaction between coherent light-emitting excitons is indeed established at the up-conversion ASE regime in $CsPbBr_3$ perovskite microrods. A positive up-conversion ΔASE phenomenon in the $CsPbBr_3$ microrods can be observed when switching from linear to circular polarization that circularly and linearly polarized with the same pump fluence generate. The positive up-conversion ΔASE phenomenon provides evidence that the coherent interaction between coherent light-emitting excitons generated through the orbit–orbit polarization interaction within coherent transition dipoles in the $CsPbBr_3$ perovskite microrods. Substantially, this result shows that the spin lifetime of orbital magnetic dipoles can reach the order of nanoseconds, which is similar to the lifetime of coherent transition dipoles in up-conversion ASE. This provides a precondition for the time constant to realize the spin alignment between coherent light-emitting excitons. Upon satisfying the time-constant precondition, spin alignment can conserve the in-phase orbital polarization and consequently introduces an additional cooperative interaction between coherent light-emitting excitons, shown as an increased up-conversion ASE. Thus, our results demonstrate a fundamental understanding of the spin alignment between coherent light-emitting excitons during up-conversion ASE action in metal halide perovskites.

Author Contributions: Conceptualization, X.Z.; methodology, X.Z.; investigation, X.Z., Y.X., and X.M.; writing—original draft preparation, X.Z.; writing—review and editing, X.Z. and X.M.; funding acquisition, X.Z. and Y.X.; X.Z. and Y.X. contributed equally to this work. All authors have read and agreed to the published version of the manuscript.

Funding: This research was funded by the Fundamental Research Funds for the Central Universities (Grant No. S21JB0100020); Project funded by China Postdoctoral Science Foundation (Grant No. 2021M690336); The National Natural Science Foundation of China (Grant No. 62104016). High-level Cultivation Program (202108404) of Huanggang Normal University: Scientific Research Project of Education Department of Hubei Province (B2021239).

Institutional Review Board Statement: Not applicable.

Informed Consent Statement: Not applicable.

Data Availability Statement: The data that supports the findings of this study are available within the article.

Acknowledgments: We acknowledge financial supports by the Fundamental Research Funds for the Central Universities (Grant No. S21JB0100020); Project funded by China Postdoctoral Science Foundation (Grant No. 2021M690336); The National Natural Science Foundation of China (Grant No. 62104016). High-level Cultivation Program (202108404) of Huanggang Normal University: Scientific Research Project of Education Department of Hubei Province (B2021239).

Conflicts of Interest: The authors declare no conflict of interest.

References

1. Snaith, H.J. Present status and future prospects of perovskite photovoltaics. *Nat. Mater.* **2018**, *17*, 372–376. [CrossRef] [PubMed]
2. Jena, A.K.; Kulkarni, A.; Miyasaka, T. Halide perovskite photovoltaics: Background, status, and future prospects. *Chem. Rev.* **2019**, *119*, 3036–3103. [CrossRef] [PubMed]
3. Zhu, H.; Fu, Y.; Meng, F.; Wu, X.; Gong, Z.; Ding, Q.; Gustafsson, M.V.; Trinh, M.T.; Jin, S.; Zhu, X. Lead halide perovskite nanowire lasers with low lasing thresholds and high quality factors. *Nat. Mater.* **2015**, *14*, 636–642. [CrossRef] [PubMed]
4. Eaton, S.W.; Lai, M.; Gibson, N.A.; Wong, A.B.; Dou, L.; Ma, J.; Wang, L.-W.; Leone, S.R.; Yang, P. Lasing in robust cesium lead halide perovskite nanowires. *Proc. Natl. Acad. Sci. USA* **2016**, *113*, 1993–1998. [CrossRef] [PubMed]
5. Lin, K.; Xing, J.; Quan, L.N.; De Arquer, F.; Gong, X.; Lu, J.; Xie, L.; Zhao, W.; Zhang, D.; Yan, C. Perovskite light-emitting diodes with external quantum efficiency exceeding 20 per cent. *Nature* **2018**, *562*, 245–248. [CrossRef] [PubMed]
6. Cho, H.; Jeong, S.-H.; Park, M.-H.; Kim, Y.-H.; Wolf, C.; Lee, C.-L.; Heo, J.H.; Sadhanala, A.; Myoung, N.; Yoo, S. Overcoming the electroluminescence efficiency limitations of perovskite light-emitting diodes. *Science* **2015**, *350*, 1222–1225. [CrossRef]
7. Dou, L.; Yang, Y.M.; You, J.; Hong, Z.; Chang, W.-H.; Li, G.; Yang, Y. Solution-processed hybrid perovskite photodetectors with high detectivity. *Nat. Commun.* **2014**, *5*, 5404. [CrossRef]
8. Tian, W.; Zhou, H.; Li, L. Hybrid organic–inorganic perovskite photodetectors. *Small* **2017**, *13*, 1702107. [CrossRef]
9. Xing, G.; Mathews, N.; Lim, S.S.; Yantara, N.; Liu, X.; Sabba, D.; Grätzel, M.; Mhaisalkar, S.; Sum, T.C. Low-temperature solution-processed wavelength-tunable perovskites for lasing. *Nat. Mater.* **2014**, *13*, 476–480. [CrossRef]
10. Filip, M.R.; Eperon, G.E.; Snaith, H.J.; Giustino, F. Steric engineering of metal-halide perovskites with tunable optical band gaps. *Nat. Commun.* **2014**, *5*, 5757. [CrossRef]
11. Xiao, Z.; Kerner, R.A.; Zhao, L.; Tran, N.L.; Lee, K.M.; Koh, T.-W.; Scholes, G.D.; Rand, B.P. Efficient perovskite light-emitting diodes featuring nanometre-sized crystallites. *Nat. Photonics* **2017**, *11*, 108–115. [CrossRef]
12. Zhang, D.; Eaton, S.W.; Yu, Y.; Dou, L.; Yang, P. Solution-phase synthesis of cesium lead halide perovskite nanowires. *J. Am. Chem. Soc.* **2015**, *137*, 9230–9233. [CrossRef] [PubMed]
13. Liu, F.; Zhang, Y.; Ding, C.; Kobayashi, S.; Izuishi, T.; Nakazawa, N.; Toyoda, T.; Ohta, T.; Hayase, S.; Minemoto, T. Highly luminescent phase-stable CsPbI3 perovskite quantum dots achieving near 100% absolute photoluminescence quantum yield. *ACS Nano* **2017**, *11*, 10373–10383. [CrossRef] [PubMed]
14. Zhang, H.; Jin, M.; Liu, X.; Zhang, Y.; Yu, Y.; Liang, X.; Xiang, W.; Wang, T. The preparation and up-conversion properties of full spectrum CsPbX 3 (X= Cl, Br, I) quantum dot glasses. *Nanoscale* **2019**, *11*, 18009–18014. [CrossRef]
15. Xu, Y.; Chen, Q.; Zhang, C.; Wang, R.; Wu, H.; Zhang, X.; Xing, G.; Yu, W.W.; Wang, X.; Zhang, Y. Two-photon-pumped perovskite semiconductor nanocrystal lasers. *J. Am. Chem. Soc.* **2016**, *138*, 3761–3768. [CrossRef]
16. Yu, Z. Effective-mass model and magneto-optical properties in hybrid perovskites. *Sci. Rep.* **2016**, *6*, 28576. [CrossRef]
17. Even, J.; Pedesseau, L.; Jancu, J.-M.; Katan, C. Importance of spin–orbit coupling in hybrid organic/inorganic perovskites for photovoltaic applications. *J. Phys. Chem. Lett.* **2013**, *4*, 2999–3005. [CrossRef]
18. Zhu, X.; Xu, H.; Liu, Y.; Zhang, J.; Wang, M.; Ivanov, I.N.; Ovchinnikova, O.S.; Hu, B. Two-Photon Up-Conversion Photoluminescence Realized through Spatially Extended Gap States in Quasi-2D Perovskite Films. *Adv. Mater.* **2019**, *31*, 1901240. [CrossRef]
19. Zhu, X.; Dai, S.-W.; Lai, Y.-L.; Dou, Y.; Wang, M.; Ho, J.-S.; Chang, Y.-A.; Chuang, Y.-T.; Lin, H.-W.; Hu, B. Packing-Shape Effects of Optical Properties in Amplified Spontaneous Emission through Dynamics of Orbit–Orbit Polarization Interaction in Hybrid Perovskite Quantum Dots Based on Self-Assembly. *J. Phys. Chem. Lett.* **2021**, *12*, 11894–11901. [CrossRef]
20. Xu, H.; Prabhakaran, P.; Choi, S.; Wang, M.; Lee, K.-S.; Hu, B. Exploring Orbit–Orbit Interaction in Relationship to Photoluminescence Quantum Efficiency in Perovskite Quantum Dots through Rashba Effect. *J. Phys. Chem. Lett.* **2019**, *11*, 1–6. [CrossRef]
21. Wang, M.; Zou, H.; Zhang, J.; Wu, T.; Xu, H.; Haacke, S.; Hu, B. Extremely Long Spin Lifetime of Light-Emitting States in Quasi-2D Perovskites through Orbit–Orbit Interaction. *J. Phys. Chem. Lett.* **2020**, *11*, 3647–3652. [CrossRef] [PubMed]
22. Zhang, J.; Qin, J.; Wu, T.; Hu, B. Doping Induced Orbit–Orbit Interaction between Excitons While Enhancing Photovoltaic Performance in Tin Perovskite Solar Cells. *J. Phys. Chem. Lett.* **2020**, *11*, 6996–7001. [CrossRef] [PubMed]
23. Cho, C.; Palatnik, A.; Sudzius, M.; Grodofzig, R.; Nehm, F.; Leo, K. Controlling and optimizing amplified spontaneous emission in perovskites. *ACS Appl. Mater. Interfaces* **2020**, *12*, 35242–35249. [CrossRef]
24. Cho, C.; Zhao, B.; Tainter, G.D.; Lee, J.-Y.; Friend, R.H.; Di, D.; Deschler, F.; Greenham, N.C. The role of photon recycling in perovskite light-emitting diodes. *Nat. Commun.* **2020**, *11*, 611. [CrossRef] [PubMed]